The Highly Expressed and Inducible Endogenous NAD(P)H:quinone Oxidoreductase 1 in Cardiovascular Cells Acts as a Potential Superoxide Scavenger

By: Hong Zhu, Zhenquan Jia, James E. Mahaney, David Ross, Hara P. Misra, Michael A. Trush, Yunbo Li

Zhu, H., Jia, Z., Mahaney, J.E., Ross, D., Misra, H.P., Trush, M.A., Li., Y., (2007). The Highly Expressed and Inducible Endogenous NAD(P)H:quinone Oxidoreductase 1 in Cardiovascular Cells Acts as a Potential Superoxide Scavenger. *Cardiovascular Toxicology*, 7(3), 202-211. doi: 10.1007/s12012-007-9001-z

The final publication is available at Springer via http://dx.doi.org/10.1007/s12012-007-9001-z

Abstract:

It has recently been demonstrated that purified NAD(P)H:quinone oxidoreductase 1 (NQO1) is able to scavenge superoxide ($O_2^{\bullet-}$) though the rate of reaction of $O_2^{\bullet-}$ with NQO1 is much lower than the rate of enzymatic dismutation catalyzed by superoxide dismutase (SOD). This study was undertaken to determine if the endogenously expressed NQO1 in cardiovascular cells could scavenge $O_2^{\bullet-}$. We observed thatNQO1 was highly expressed in cardiovascular cells, including rat aortic smooth muscle A10 and cardiac H9c2 cells, as well as normal human aortic smooth muscle and endothelial cells. NQO1, but not SOD in the cardiovascular cells was highly inducible by 3*H*-1,2-dithiole-3-thione (D3T). Cytosols from H9c2 and human aortic smooth muscle cells (HASMCs) were isolated to determine the $O_2^{\bullet-}$ scavenging ability of the endogenously expressed NQO1 by using pyrogallol autooxidation assay. We showed that cytosols from the above cells inhibited pyrogallol autooxidation in an NADPH or NADH-dependent manner. The NADH/NADPH-dependent inhibition of pyrogallol autooxidation by the cytosols was completely abolished by the NQO1-specific inhibitor, ES936, suggesting that the endogenously expressed NQO1 could scavenge $O_2^{\bullet-}$. In the presence of NADH/NADPH, cytosols from D3T-treated cells showed increased ability to scavenge $O_2^{\bullet-}$ as compared to cytosols from untreated cells. This increased ability to scavenge $O_2^{\bullet-}$ was also completely reversed by ES936. 5-(Diethoxyphosphoryl)-5-methyl-1-pyrroline-*N*-oxide spin-trapping experiments using potassium superoxide as a $O_2^{\bullet-}$ generator further confirmed the ability of NQO1 from HASMCs to scavenge $O_2^{\bullet-}$. The spin-trapping experiments also showed that induction of NQO1 by D3T in HASMCs augmented the $O_2^{\bullet-}$ scavenging ability. Taken together, these results demonstrate that the highly expressed and inducible endogenous NQO1 in cardiovascular cells may act as a potential $O_2^{\bullet-}$ scavenger.

Abbreviations

D3T: 3*H*-1,2-Dithiole-3-thione
DCIP: 2,6-Dichloroindophenol
DEPMPO: 5-(Diethoxyphosphoryl)-5-methyl-1-pyrroline-*N*-oxide
EPR: Electron paramagnetic resonance
FBS: Fetal bovine serum
HASMCs: Human aortic smooth muscle cells
KO_2: Potassium superoxide
NQO1: NAD(P)H:quinone oxidoreductase 1
$O_2^{\bullet-}$: Superoxide
PBS: Phosphate-buffered saline
ROS: Reactive oxygen species
RT-PCR: Reverse transcriptase-polymerase chain reaction
SOD: Superoxide dismutase

Keywords: NAD(P)H:quinone oxidoreductase 1 | Cardiovascular cells | 3*H*-1,2-dithiole-3-thione | Superoxide Spin-trapping

Article:

Introduction

NAD(P)H:quinone oxidoreductase 1 (NQO1), also referred to as DT-diaphorase, is a flavoprotein that catalyzes the two-electron reduction of quinones and quinoid compounds to hydroquinones, using either NADH or NADPH as the electron donor [*1*]. The two-electron reduction of redox-active quinones by NQO1 to hydroquinones also bypasses the formation of semiquinone radicals via one-electron reduction, and thus limiting the formation of reactive oxygen species (ROS) [*1*]. NQO1 may also play an antioxidative role via reduction of cellular quinone compounds, such as vitamin E quinone and ubiquinone to the hydroquinone forms that possess excellent antioxidative properties [*2*, *3*]. The notion that NQO1 may act as an antioxidative protein is further strengthened by the observations that cellular NQO1 is highly inducible by authentic ROS or under conditions that are known to form ROS, such as radiation and redox cycling compounds [*4–6*]. In addition to the above antioxidative properties, NQO1 has been shown to play an important part in regulating the stability of p53 protein via direct protein–protein interaction [*7, 8*]. p53 protein is a redox-responsive transcription factor that upregulates a number of proteins involved in protection against oxidative stress, including glutathione peroxidase as well as proteins with homology to quinone oxidoreductase/NQO1 [*9–11*].

The above findings suggest that NQO1 may play a broader role in protecting cells against oxidative insults. In this context, Siegel et al. have recently reported that purified human recombinant NQO1 is able to scavenge superoxide ($O_2^{\bullet-}$) using NADH or NADPH as the electron donor [*12*]. It has further been demonstrated that cytosols derived from NQO1-

transfected cells are able to scavenge $O_2^{\bullet-}$ in an NQO1-dependent manner [*12*]. However, the rate of reaction of $O_2^{\bullet-}$ with NQO1 is in the order of 4 orders of magnitude less than the rate of enzymatic dismutation catalyzed by superoxide dismutase (SOD) [*12*]. This observation implies that in the presence of SOD, the significance of endogenous NQO1 in scavenging $O_2^{\bullet-}$would be determined by its levels/activities in the cells. Although NQO1 is a ubiquitously expressed protein found in various mammalian tissues and cells, its levels of expression vary among different tissues/cells [*1*,*13*, *14*]. In this regard, we previously observed that NOQ1 was highly expressed in cardiovascular tissues, including mouse myocardium [*15*] and human aortic tissue [*14*], as well as in the rat cardiac line, H9c2 cells [*16*]. In the present study, we further observed that NQO1 was highly expressed constitutively in rat aortic smooth muscle A10 cells, as well as in normal human aortic smooth muscle and endothelial cells, where expression of SOD was relatively low as compared to most other types of cells. The endogenous NQO1, but not SOD in the above cardiovascular cells was also highly inducible by 3*H*-1,2-dithiole-3-thione (D3T). Moreover, we demonstrated that the highly expressed and inducible endogenous NQO1 from cardiovascular cells was able to scavenge $O_2^{\bullet-}$, and might act as an important endogenous defense against $O_2^{\bullet-}$.

Materials and Methods

Chemicals and Materials

D3T with a purity of 99.8% was generously provided by Dr. Mary Tanga at SRI International (Menlo Park, CA) and Dr. Linda Brady at National Institute of Mental Health (Bethesda, MD). RPMI 1640 medium, Dulbecco's modified Eagle's medium (DMEM), Ham's F12 medium, penicillin, streptomycin, fetal bovine serum (FBS), horse serum, and Dulbecco's phosphate-buffered saline (PBS) were from Gibco-Invitrogen (Carlsbad, CA). 5-Methoxy-1,2-dimethyl-3-[(4-nitrophenoxy)methyl]indole-4,7-dione (ES936), a potent and specific inhibitor of NQO1 was synthesized as described previously [*17*]. Anti-NQO1 and β-actin antibodies were from Santa Cruz Biotech (Santa Cruz, CA). 5-(Diethoxyphosphoryl)-5-methyl-1-pyrroline-*N*-oxide (DEPMPO) was from Calbiochem (San Diego, CA). Endothelial cell growth supplement (ECGS) was from Upstate (Charlottesville, VA). All other chemicals and agents were from Sigma Chemical (St. Louis, MO).

Cell Culture and Cytosol Preparation

Rat aortic smooth muscle A10 and cardiac H9c2 cells (ATCC, Manasas, VA) were cultured in DMEM supplemented with 10% FBS, 100 U/ml penicillin, and 100 μg/ml streptomycin, as described before [*16*, *18*]. Normal human aortic smooth muscle cells (ATCC) were cultured in Ham's F12 medium supplemented with 10% FBS, 0.01 mg/ml insulin, 0.01 mg/ml transferin, 10 ng/ml sodium selenite, 0.03 mg/ml ECGS, 100 U/ml penicillin, and 100 μg/ml streptomycin, as described before [*19*]. Normal human aortic endothelial cells (ATCC) were cultured in Ham's F12 medium supplemented with 10% FBS, 0.1 mg/ml heparin, 0.03 mg/ml ECGS, 100 U/ml

penicillin, and 100 μg/ml streptomycin. Primary bone marrow stromal cells were isolated from ICR/Sv129 mice and cultured in RPMI 1640 medium supplemented with 7.5% FBS, 7.5% horse serum, 50 μM 2-mercaptoethanol, 0.1 mg/ml pyruvate, 100 U/ml penicillin, and 100 μg/ml streptomycin, as described before [*20*]. Peritoneal macrophages were isolated from ICR/Sv129 mice following intraperitoneal injection of 4% thioglycollate medium, and cultured in RPMI 1640 medium supplemented with 10% FBS, 100 U/ml penicillin, and 100 μg/ml streptomycin. Rat insulin-secreting RINm5F cells (ATCC) were cultured in RPMI 1640 medium supplemented with 10% FBS, 100 U/ml penicillin, and 100 μg/ml streptomycin, as described before [*21*]. Human neuronal SH-Sy5y and intestinal Caco-2 cells (ATCC) were cultured in DMEM supplemented with 10% FBS, 100 U/ml penicillin, and 100 μg/ml streptomycin. For cytosol preparation, cells were harvested and washed with PBS. The cell pellets were resuspended in 10 mM Tris–HCl buffer, pH 7.4, containing 250 mM sucrose, sonicated on ice for 5 s, and followed by centrifugation at 30,000 g for 15 min to remove insoluble matter, as described before [*12*]. The resulting supernatants were collected and the protein concentrations were measured with a Bio-Rad protein assay kit (Hercules, CA) using bovine serum albumin as the standard.

Measurement of Cellular NQO1 Activity

Cellular NQO1 activity was determined using dichloroindophenol (DCIP) as the two-electron acceptor, as described before [*16*]. In brief, the reaction mix contained in 50 mM Tris–HCl, pH 7.5, 0.08% Triton X-100, 0.25 mM NADPH, 80 μM 2,6-dichloroindophenol (DCIP) in the presence or absence of 60 μM dicumarol. To an assay cuvette, 0.695 ml of reaction mix was added. The reaction was started by adding 5 μl of sample, and the two-electron reduction of DCIP was monitored at 600 nm, 25°C for 3 min. The dicumarol-inhibitableNQO1 activity was calculated using the extinction coefficient of 21.0 mM^{-1} cm^{-1}, and expressed as nmol of DCIP reduced per min per mg of cellular protein.

Measurement of Cellular SOD Activity

SOD activity was determined by the method of Spitz and Oberley [*22*] with slight modifications. In brief, the reaction mix contained in 50 mM potassium phosphate buffer, pH 7.8, 1.33 mM diethylenetriaminepentaacetic acid (DTPA), 1.0 U/ml catalase, 70 μM nitroblue tetrazolium, 0.2 mM xanthine, 50 μM bathocuproinedisulfonic acid, and 0.13 mg/ml bovine serum albumin. About 0.8 ml of the reaction mix was added to each cuvette, followed by addition of 100 μl of sample. The cuvettes were pre-warmed at 37°C for 3 min. The reaction was then initiated by adding 100 μl of xanthine oxidase (0.1–0.2 U/ml). The formation of formazan blue was monitored at 560 nm, 37°C for 5 min. Sample SOD activity was calculated using a concurrently run SOD (Sigma) standard curve, and expressed as units per mg of cellular protein.

Immunoblot Analysis

Prior to electrophoresis, the samples were diluted with 4x sample loading buffer (62.5 mM Tris–HCl, pH 6.8, 10% glycerol, 2% SDS, 5% 2-mercaptoethanol, and 0.05% bromophenol blue) and heated at 95°C for 5 min. Equal amounts of protein from each sample were resolved by SDS-PAGE on 10% gels, transferred electrophoretically to a nitrocellulose membrane (Amersham, Piscataway, NJ). The membrane was blocked with 5% non-fat dried milk in TTBS buffer containing 20 mM Tris–HCl, pH 7.4, 150 mM NaCl, and 0.05% Tween-20 at room temperature for 1.5 h. The membrane was incubated with primary antibodies overnight at 4°C, followed by washing in TTBS buffer. The membrane was then incubated with horseradish peroxidase-labeled secondary antibodies (Santa Cruz Biotech) for 1.5 h, followed by washing in TTBS buffer. The membrane was visualized using an enhanced chemiluminescence system (Amersham) and blots were quantified by Gel-Pro Analyzer version 4.5 (MediaCybernetics, Silver Spring, MD).

Reverse Transcriptase-Polymerase Chain Reaction (RT-PCR) Analysis

Total RNA from cells was extracted using Trizol reagent (Invitrogen) following the manufacturer's instruction.cDNA synthesis and subsequent PCR reaction were performed using Superscript II One-Step system (Invitrogen) in a volume of 25 μl according to manufacturer's instruction. The cycling conditions for RT-PCR were the following: 50°C for 30 min (reverse transcription), 94°C for 2 min (pre-denaturation), followed by 25 cycles of PCR amplification process including denaturing at 94°C for 15 s, annealing at 57°C for 30 s, and extension at 72°C for 45 s, and by 1 cycle of final extension at 72°C for 10 min. PCR primers were synthesized by the DNA/RNA Synthesis Core Facility of The Johns Hopkins University (Baltimore, MD). PCR products were separated by 1% agarose gel electrophoresis. Gels were stained with 0.5 μg/ml solution of ethidium bromide for 30 min followed by another 30 min destaining in water. The gels were then analyzed under ultraviolet light using an Alpha Innotech Imaging system (San Leandro, CA). Various amounts of total RNA were used to demonstrate a linear amplification of the specific mRNA. The quantitative capacity of RT-PCR in detecting mRNA levels has previously been characterized by our laboratory and others [*21*, *23*].

Pyrogallol Autooxidation Assay

Inhibition of pyrogallol autooxidation was performed according to the procedures described before [*12*]. Briefly, the reaction mix contained in 50 mM Tris–HCl, pH 8.0, 2 mM EDTA, 0.2 mM NADH or NADPH, cytosol (25 μg protein) in the presence or absence of 2.5 μM ES936. The reaction was started by adding pyrogallol (prepared freshly in ice-cold de-ionized water) to give a final concentration of 0.2 mM. The autooxidation of pyrogallol was monitored at 420 nm, 27°C for 5 min.

Electron Paramagnetic Resonance (EPR) Spin-Trapping Assay

For DEPMPO spin-trapping measurement of $O_2^{\bullet -}$, EPR spectra were recorded at room temperature with a spectrometer (Bruker D-200 ER, IBM-Bruker), operating at X-band with a TM cavity, as described previously [*24*]. The EPR parameters were set at 100 KHz, X band

microwave frequency, 9.5 GHz; microwave power, 20 mW (milliwatts); modulation amplitude, 1 G (gauss); time constant, 160 s; scan time, 50 s; and receiver gain, 5×10^5. The reaction mix contained in PBS, pH 7.4, 0.1 mM DTPA, 0.2 mM NADH, cytosol (25 μg protein), and 10 mM DEPMPO in the presence or absence of 2.5 μM ES936. The reaction was started by addition of potassium superoxide (KO_2) (prepared freshly in anhydrous dimethyl sulfoxide), and the reaction mixture was then immediately transferred to a capillary tube for EPR measurement at room temperature. Spectral simulations were performed on the EPR data by matching directly to the spectra as described previously [*24*].

Statistical Analyses

All data are expressed as means ± SEM from at least three separate experiments. Differences between mean values of multiple groups were analyzed by one-way analysis of variance (ANOVA) followed by Student–Newman–Keuls test. Differences between two groups were analyzed by Student *t*-test. Statistical significance was considered at $P < 0.05$.

Results

Constitutive Expression of NQO1 in Various Types of Cells

NQO1 is a ubiquitously distributed cellular protein in mammals [*1*]. Both the basal expression and/or the chemical inducibility of NQO1 in various cells have been investigated by our laboratories over the last several years. Figure 1 shows the constitutive levels of NQO1 in nine different types of cells used in our laboratories. Notably, the basal levels of NQO1 in rat aortic smooth muscle A10 and cardiac H9c2 cells, as well as in normal human aortic smooth muscle and endothelial cells were much higher than those in other types of cells, including mouse bone marrow stromal cells, mouse peritoneal macrophages, rat insulin-secreting RINm5F, human SH-Sy5y cells, and human Caco-2 cells. Based on the assay of dicumarol-inhibitable DCIP reduction, levels of NQO1 in the five types of non-cardiovascular cells ranged from barely detectable to ~50 nmol DCIP/min/mg protein, whereas its levels in the four types of cardiovascular cells ranged from ~500 to ~1000 nmol DCIP/min/mg protein (Fig. 1). Such high constitutive levels of cellular NQO1 have not been reported for other types of cells in literature.

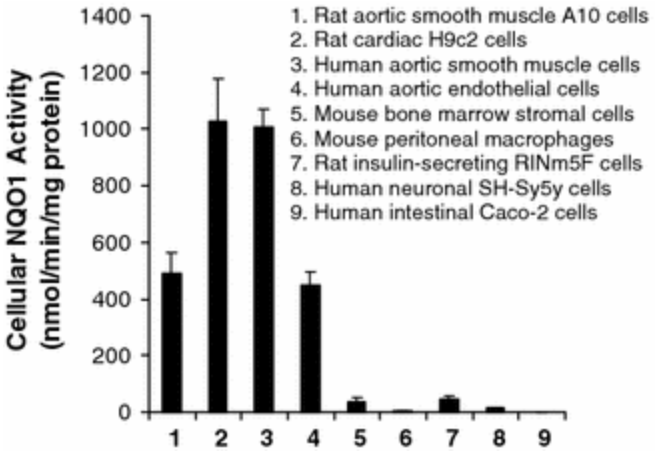

Fig. 1 Constitutive levels of NQO1 in various types of cells. Cells were cultured and cellular NQO1 activity was measured as described in the Materials and Methods section. Values represent mean ± SEM (n = 3–6)

Induction of Endogenous NQO1 by D3T in Cardiovascular Cells

NQO1 is known for its inducibility under various conditions, including exposure to quinone compounds, oxidative stress, and chemoprotectants [*4–6*]. As shown in Fig. 2, the highly expressed endogenous NQO1in the four types of cardiovascular cells examined was also highly inducible by D3T. Induction of NQO1 by D3T exhibited a concentration- and time-dependent manner. Incubation of rat cardiac H9c2 or human aortic smooth muscle cells (HASMCs) with various concentrations of D3T for 48 h also led to significant induction of NQO1 protein expression, as detected by immunoblot analysis (Fig. 3). In line with the increases of NQO1 activity shown in Fig. 2, induction of NQO1 protein expression by D3T in H9c2 cells and HASMCs also showed a concentration-dependent manner. The similar extent of induction of NQO1 activity (Fig. 2) and protein expression (Fig. 3) by D3T in H9c2 and HASMCs suggested that induction of NQO1 activity by D3T shown in Fig. 2 was due to its increased protein expression. Figure 4 shows time-dependent increases in the levels of NQO1 mRNA following incubation of H9c2 and HASMCs with D3T. As shown, a significant increase in the levels of NQO1 mRNA was observed 1 h after D3T treatment in both types of cells. In H9c2 cells, mRNA levels peaked at 12 and 24 h after D3T treatment, and declined at 48 h though the mRNA level at 48 h was still significantly higher than that at 0 h of D3T treatment (Fig. 4A). Notably, mRNA levels for NQO1 in HASMCs continued to increase from 1 to 48 h following D3T treatment (Fig. 4B), suggesting sustained induction of NQO1 gene expression by D3T in HASMCs. Recently, Nrf2 signaling has been shown to be critically involved in the transcriptional activation of NQO1 gene by D3T in various types of cells, including mouse cardiac fibroblasts and bone marrow stromal cells [*20*, *25*]. It is likely that Nrf2 signaling may also be involved in the upregulation of NQO1 by D3T in rat cardiac H9c2 cells as well as HASMCs.

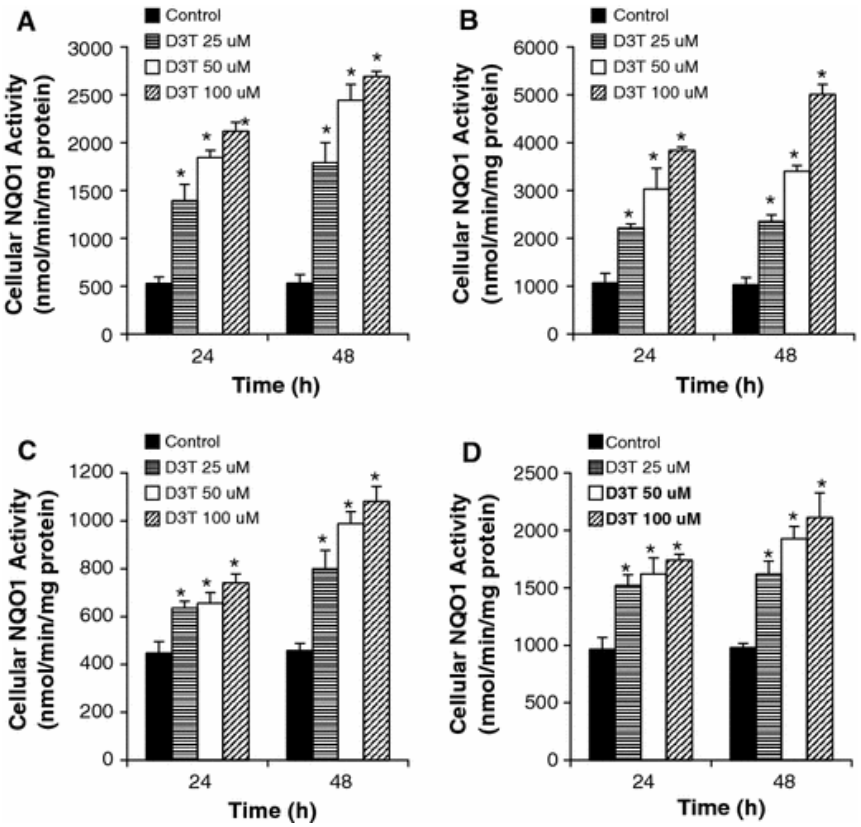

Fig. 2 Induction of NQO1 by D3T in cardiovascular cells. (Panel **A**), rat aortic smooth muscle A10 cells; (panel **B**), rat cardiac H9c2 cells; (panel **C**), human aortic endothelial cells; (panel **D**), human aortic smooth muscle cells. Cells were incubated with the indicated concentrations of D3T for 24 and 48 h, followed by measurement of cellular NQO1, as described in the Materials and Methods section. Values represent mean ± SEM (n = 3–6). *, significantly different from control

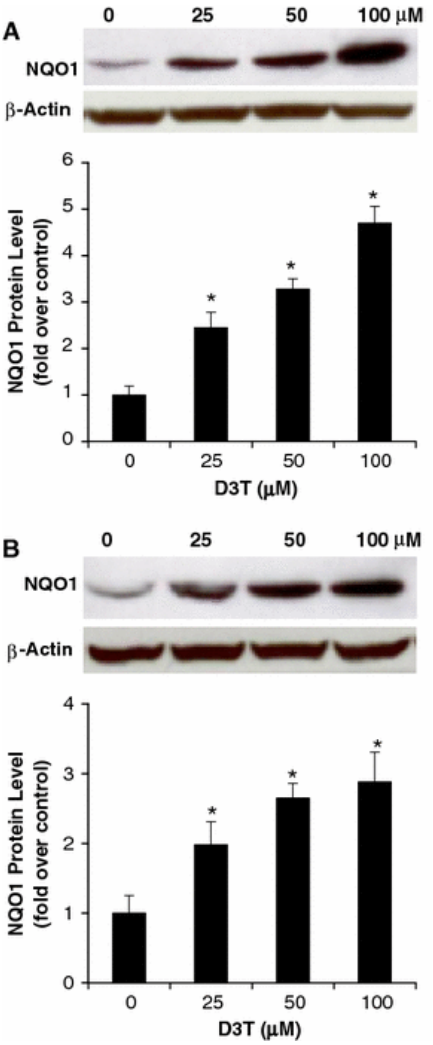

Fig. 3 Induction of NQO1 protein expression by D3T in rat cardiac H9c2 cells (panel **A**) and human aortic smooth muscle cells (panel **B**). Cells were incubated with the indicated concentrations of D3T for 48 h, followed by immunoblot detection of cellular NQO1 protein expression, as described in the Materials and Methods section. Values represent mean ± SEM (n = 3–4). *, significantly different from control. β-Action serves as a sample loading control

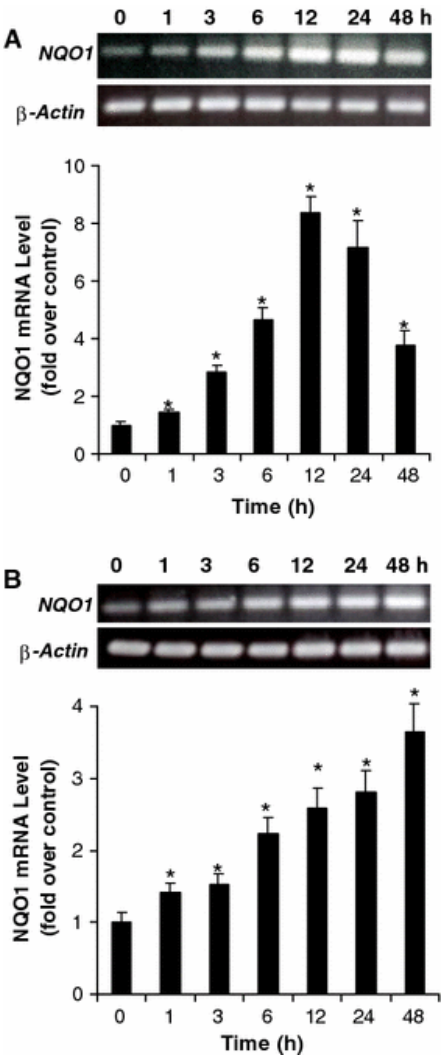

Fig. 4 Induction of NQO1 mRNA expression by D3T in rat cardiac H9c2 cells (panel **A**) and human aortic smooth muscle cells (panel **B**). Cells were incubated with 100 μM D3T for the indicated time points, followed by RT-PCR detection of the levels of NQO1 mRNA, as described in the Materials and Methods section. Values represent mean ± SEM (n = 3). *, significantly different from 0 h. β-Action serves as a sample loading control

In contrast to the high basal expression as well as D3T-inducibility of NOQ1, the constitutive levels of SOD were relatively low in H9c2 and HASMCs (Table 1). In addition, SOD in neither type of the cells was inducible by D3T under the present experimental conditions (Table 1).

Table 1 Basal levels of SOD and NQO1, and their differential inducibility by D3T in rat cardiac H9c2 and human aortic smooth muscle cells (HASMCs). Cells were incubated with 100 μM D3T for 48 h, followed by measurement of the activity of SOD and NQO1, as described in the Materials and Methods section

Cell type	SOD (units/mg protein)	NQO1(nmol/min/mg protein)
H9c2 cells	10.4 ± 1.4	1030 ± 150
HASMCs	4.5 ± 0.5	978 ± 38
H9c2 cells + D3T	9.6 ± 1.4	5007 ± 211
HASMCs + D3T	4.3 ± 0.4	2112 ± 214

Values represent mean ± SEM (n = 3–4)

Inhibition of Pyrogallol Autooxidation by Endogenous NQO1 from Cardiovascular Cells

Since rat cardiac H9c2 cells and HASMCs showed the highest levels of NQO1, we selected these two types of cells to further determine if the endogenously expressed NQO1 could scavenge $O_2^{\bullet-}$. To this end, pyrogallol autooxidation assay was used to determine the $O_2^{\bullet-}$ scavenging capacity of NQO1 from H9c2 cells and HASMCs. As shown in Fig. 5, in the absence of NADH or NADPH, cytosol from control H9c2 cells inhibited pyrogallol autooxidation apparently due to the presence of SOD in the cytosol. Addition of NADH or NADPH led to further inhibition of pyrogallol autooxidation by the cytosol. This increased inhibition of pyrogallol autooxidation was completely abolished by the NQO1 specific inhibitor, ES936 [*26*]. In the absence of NADH or NADPH, cytosol from D3T-treated H9c2 cells inhibited pyrogallol autooxidation to the same extent as that observed with cytosol from control H9c2 cells (Fig. 5). Notably, in the presence of NADH or NADPH cytosol from D3T-treated H9c2 cells showed increased ability of inhibiting pyrogallol autooxidation as compared to cytosol from control H9c2 cells. Similarly, this increased inhibition of pyrogallol autooxidation was completely reversed by ES936 (Fig. 5). As shown, NADH or NADPH alone did not significantly affect the autooxidation of pyrogallol. It was also observed that the presence of ES936 (2.5 μM) alone did not affect the autooxidation of pyrogallol (data not shown). It is worthy of mentioning that ES936 at concentrations inhibiting more than 95% of cellular NQO1 activity does not affect cell viability, alter cellular levels of acid-soluble thiols, or inhibit other cellular reductases [*26*].

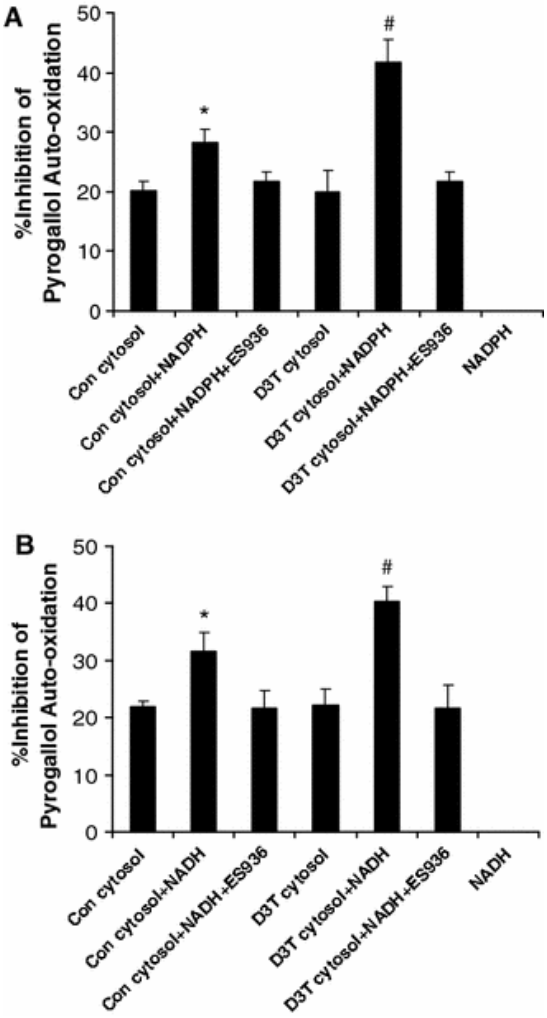

Fig. 5 Inhibition of pyrogallol autooxidation by cytosols from H9c2 cells. Pyrogallol autooxidation was determined after addition of cytosols, and NADPH (panel **A**), or NADH (panel **B**) in the presence or absence of ES936, as described in the Materials and Methods section. “Con cytosol” refers to the cytosol isolated from control H9c2 cells; “D3T cytosol” refers to the cytosol isolated from H9c2 cells after treatment with 100 μM D3T for 48 h. Values represent mean ± SEM (n = 3–5). In both panels A and B, *, significantly different from “Con cytosol”; In panel A, #, significantly different from “Con cytosol + NADPH”; In panel B, #, significantly different from “Con cytosol + NADH”

Consistent with what observed with H9c2 cytosol, cytosol from HASMCs inhibited autooxidation of pyrogallol in an NADH-dependent manner. This NADH-dependent inhibition of pyrogallol autooxidation by cytosol from HASMCs was also completely abolished by ES936. Similarly, cytosol from D3T-treated HASMCs exhibited increased ability of NADH-dependent inhibition of pyrogallol autooxidation, as compared to cotosol from control HASMCs (Fig. 6). In contrast to what we observed using cytosols from HASMCs as well as H9c2 cells, cytosols from cells expressing low levels of NQO1 (~40–50 nmol DCIP/min/mg protein), including mouse

bone marrow stromal cells and rat RINm5F cells (Fig. 1), did not exert any significant NAD(P)H-dependent inhibition of pyrogallol autooxidation (data not shown). The levels of SOD in these cells were similar to those in HASMCs [*20*, unpublished observations].

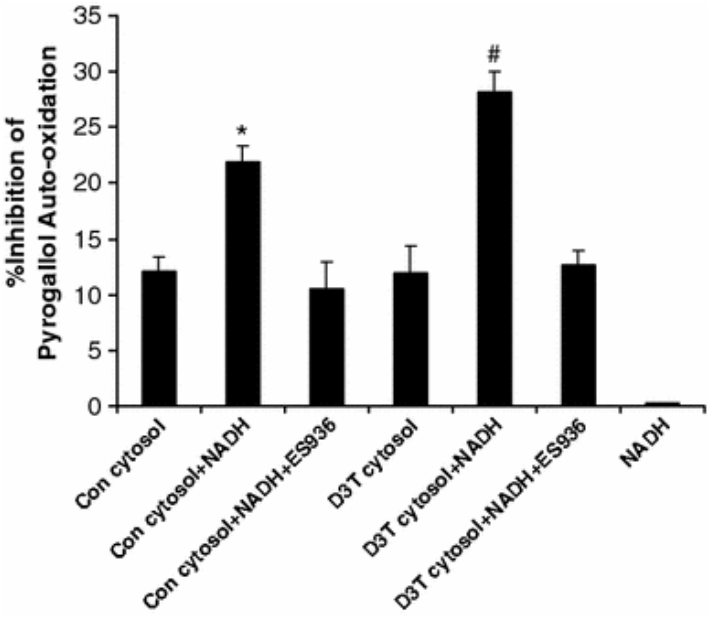

Fig. 6 Inhibition of pyrogallol autooxidation by cytosols from human aortic smooth muscle cells (HASMCs). Pyrogallol autooxidation was determined after addition of cytosols and NADH in the presence or absence of ES936, as described in the Materials and Methods section. "Con cytosol" refers to the cytosol isolated from control HASMCs; "D3T cytosol" refers to the cytosol isolated from HASMCs after treatment with 100 μM D3T for 48 h. Values represent mean ± SEM (n = 3–5). *, significantly different from "Con cytosol"; #, significantly different from "Con cytosol + NADH"

DEPMPO Spin-Trapping Detection of $O_2^{\bullet-}$ Scavenging Ability of Endogenous NQO1 from HASMCs

DEPMPO-spin trapping technique was used to further determine the $O_2^{\cdot-}$ scavenging ability of the endogenous NQO1 from HASMCs. As shown in Fig. 7A, reaction of DEPMPO with KO_2 resulted in the formation of a single DEPMPO-superoxide (DEPMPO-OOH) spin-adduct, indicating the generation of $O_2^{\cdot-}$ in the system. In the absence of NADH, addition of cytosol from control HASMCs caused a significant decrease in the levels of $O_2^{\cdot-}$ generated from KO_2. The combination of NADH and cytosol caused a further decrease in the levels of $O_2^{\cdot-}$, which was completely reversed by ES936. In the absence of NADH, cytosol from D3T-treated HASMCs caused a decrease in the level of $O_2^{\cdot-}$, similar to that seen with cytosol from control HASMCs (Fig. 7). Notably, combination of NADH and cytosol from D3T-treated HASMCs led to much larger decrease in the levels of $O_2^{\bullet-}$, as compared to the combination of NADH and cytosol from control HASMCs (Fig. 7). The NADH-dependent $O_2^{\bullet-}$ scavenging capacity of

cytosol from D3T-treated HASMCs was completely reversed by ES936 (Fig. 7). Neither NADH nor ES936 significantly affected the formation of DEPMPO-OOH adduct (Fig. 7; data not shown).

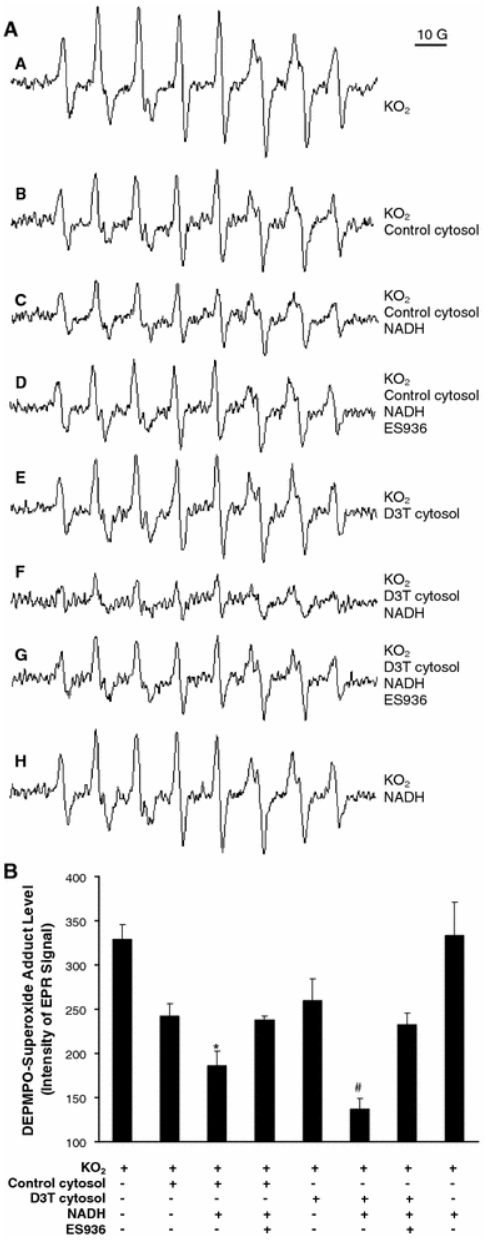

Fig. 7 Inhibition of DEPMPO-OOH adduct formation by cytosols from human aortic smooth muscle cells (HASMCs). Formation of DEPMPO-OOH adduct was detected by EPR after incubation of DEPMPO/$KO_2$with cytosols and NADH in the presence or absence of ES936, as described in the Materials and Methods section. “Control cytosol” refers to the cytosol isolated from control HASMCs; “D3T cytosol” refers to the cytosol isolated from HASMCs after treatment with 100 μM D3T for 48 h. Panel (**A**) shows representative EPR spectra; Values in

panel (**B**) represent mean ± SEM (n = 4–7). *, significantly different from "KO_2 + Control cytosol"; #, significantly different from "KO_2 + Control cytosol + NADH"

Discussion

The much lower reaction rate constant between NQO1 and $O_2^{\bullet-}$ as compared to that between SOD and $O_2^{\bullet-}$ [*12*] implies that in order for NQO1 to scavenge $O_2^{\bullet-}$ in a cellular environment with SOD, it needs to be present at high levels. Indeed, as described in the Results section, cytosols from cells expressing low levels of NQO1 (~40–50 nmol DCIP/min/mg protein) did not exhibit any significant NQO1-dependent ability of scavenging $O_2^{\bullet-}$. The present study demonstrated that cardiovascular cells, including rat aortic smooth muscle A10, cardiac H9c2 cells, as well as normal human aortic smooth muscle and endothelial cells expressed constitutively high levels of NQO1 (~500–1000 nmol DCPI/min/mg protein). The high basal levels of NQO1 in normal human aortic smooth muscle and endothelial cells observed in the present study are in line with a previous report by Siegel et al. showing that human aortic tissue expresses high levels of NQO1 protein [*14*]. While the significance for the presence of high levels of NQO1 in cardiovascular tissue/cells remains to be fully understood, one possibility could be that the highly expressed endogenous NQO1 in cardiovascular tissue/cells could act as a potential defense mechanism for $O_2^{\bullet-}$. In this context, levels of SOD is relatively low in cardiovascular tissue/cells [*6*, *27*, Table 1]. The results of the present study further demonstrated that the endogenously expressed NQO1 from cardiovascular cells could scavenge $O_2^{\bullet-}$generated from two different sources, i.e., pyrogallol autooxidation and KO_2.

In an alkaline environment, pyrogallol autooxidizes and generates $O_2^{\bullet-}$, which in turn propagates the autooxidation process [*28*, *29*]. Scavengers of $O_2^{\bullet-}$ are able to inhibit the autooxidation of pyrogallol, and as such pyrogallol autooxidation assay is widely used to detect SOD activity or the capacity of other $O_2^{\bullet-}$scavenging compounds [*28*, *29*]. In the absence of exogenously added NADH or NADPH, inhibition of pyrogallol autooxidation by cytosols as shown in Figs. 5 and 6 was apparently due to the presence of SOD in the cytosols. Since SOD was not induced by D3T, cytosols from control cells versus D3T-treated cells showed the same capacity of inhibiting pyrogallol autooxidation in the absence of NADH or NADPH (Figs. 5 and 6). The NADH- or NADPH-dependent inhibition of pyrogallol autooxidation by cytosols was completely reversed by the NQO1 specific inhibitor, ES936, suggesting that the endogenously expressed NQO1 could scavenge $O_2^{\bullet-}$. This notion was further strengthened by the observation that in the presence of NADH or NADPH cytosol from D3T-treated cells showed increased capacity of inhibiting pyrogallol autooxidation as compared to cytosol from control cells (Figs. 5 and 6). As shown in Table 1, D3T treatment led to induction of NQO1 but not SOD in H9c2 and HASMCs. Notably, the increased inhibition of pyrogallol autooxidation by cytosol from D3T-treated cells was not proportionally related to the induction of cellular NQO1 by D3T (Figs. 5 and 6, Table 1). For example, D3T treatment led to a ~5-fold induction of NQO1 in H9c2 cells, but the NADH/NADPH-dependent %inhibition of pyrogallol autooxidation by the

cytosol was only augmented by ~2–2.5-fold. Similarly, the 2-fold induction of NQO1 by D3T in HASMCs led to a less than 2-fold increase in the %inhibition of pyrogallol autooxidation (Fig. 6). While the exact reason for the above discrepancy remains unknown, one possibility was that D3T might induce some cellular enzymes, which could potentially interfere with pyrogallol autooxidation.

To further demonstrate the ability of endogenous NQO1 from cardiovascular cells to scavenge $O_2^{\bullet-}$, $KO_2$was used as another source of $O_2^{\bullet-}$, and the levels of $O_2^{\bullet-}$ were detected by DEPMPO spin-trapping. EPR spin-trapping in conjunction with KO_2 provides more definitive evidence for the ability of $O_2^{\bullet-}$scavengers. Using this technique, Siegel et al. [*12*] have demonstrated that purified NQO1 scavenges $O_2^{\bullet-}$in an NADH-dependent manner. They have further shown that the ability of purified NQO1 plus NADH to scavenge $O_2^{\bullet-}$ is completely diminished in the presence of ES936 [*12*]. As shown in Fig. 7, in the absence of NADH, cytosol from HASMCs decreased the formation of DEPMPO-OOH adduct, indicating the ability of scavenging $O_2^{\bullet-}$. This observation is in line with the results obtained with the pyrogallol autooxidation assay (Figs. 5 and 6). Addition of NADH to cytosol from control HASMCs further decreased the formation of DEPMPO-OOH adduct, and this NADH-dependent effect was completely reversed by ES936, suggesting that the endogenous NQO1 from HASMCs was able to significantly scavenge $O_2^{\bullet-}$. Notably, the decrease in the formation of DEPMPO-OOH adduct by NQO1 was similar to that caused by SOD (i.e., cytosol in the absence of NADH). This observation suggested that in HASMCs NQO1 and SOD might play an equally important part in scavenging $O_2^{\bullet-}$. Although the reaction rate constant between NQO1 and $O_2^{\bullet-}$ is much lower than that between SOD and $O_2^{\bullet-}$, the extremely high levels of NQO1 plus the relative deficiency of SOD in HASMCs (Table 1) would make it possible for NQO1 to play an important part in scavenging $O_2^{\bullet-}$. As shown, cytosol from D3T-treated HASMCs decreased the formation of DEPMPO-OOH adduct to the same extent as that seen with control HASMC-derived cytosol (Fig. 7). This observation is consistent with the results in Table 1, showing that D3T treatment did not affect the levels of SOD in HASMCs. In contrast, in the presence of NADH cytosol from D3T-treated HASMCs caused a further remarkable decrease in the formation of DEPMPO-OOH adduct, and this effect was completely reversed by ES936 (Fig. 7). This result suggested that induction of NQO1 by D3T in HASMCs could lead to an enhanced ability of scavenging $O_2^{\bullet-}$. Notably, the enhanced $O_2^{\bullet-}$ scavenging ability by NQO1 (Fig. 7) was proportionally related to the extent of induction of this enzyme by D3T in HASMCs (Table 1), further supporting the notion that the highly expressed and inducible NQO1 in HASMCs could act as an important $O_2^{\bullet-}$ scavenger.

In summary, the results of the present study demonstrate that NQO1 is highly expressed and inducible in cardiovascular cells where SOD expression is relatively low, and that the endogenously expressed NQO1from cardiovascular cells appears to act as an important scavenger for $O_2^{\bullet-}$. These results are also in line with the early study by Siegel et al., showing that purified recombinant human NQO1 as well as cytosols from NQO1-transfected cells posses

NAD(P)H-dependent $O_2^{\bullet-}$ scavenging activity [*12*]. These results also suggest that the endogenously expressed NQO1 in cardiovascular cells, including normal human vascular smooth muscle and endothelial cells may be an important defense mechanism for $O_2^{\bullet-}$. The significance for cardiovascular cellular NQO1 to act as a potentially important defense mechanism for $O_2^{\bullet-}$ is further strengthened by the observation that induction of NQO1 by D3T augments its ability of scavenging $O_2^{\bullet-}$(Fig. 7). In this context, as stated above, NQO1 is known for its high inducibility by chemoprotectants as well as under various stress conditions [*4–6*].

Acknowledgments

This work was supported in part by NIH R01 HL71190 (YL). HZ and ZJ contributed equally.

References

1. Ross, D. (2004). Quinone reductases multitasking in the metabolic world. *Drug Metabolism Reviews, 36,* 639–654.

2. Siegel, D., Bolton, E. M., Burr, J. A., Liebler, D. C., & Ross, D. (1997). The reduction of alpha-tocopherolquinone by human NAD(P)H:quinone oxidoreductase: The role of alpha-tocopherolhydroquinone as a cellular antioxidant. *Molecular Pharmacology, 52,* 300–305.

3. Beyer, R. E., Segura-Aguilar, J., di Bernardo, S., Cavazzoni, M., Fato, R., Fiorentini, D., Galli, M. C., Setti, M., Landi, L., & Lenaz, G. (1997). The two-electron quinone reductase DT-diaphorase generates and maintains the antioxidant (reduced) form of coenzyme Q in membranes. *Molecular Aspects of Medicine*, *18*(Suppl), S15–S23.

4. Agrawal, A., Choudhary, D., Upreti, M., Rath, P. C., & Kale, R. K. (2001). Radiation induced oxidative stress: I. Studies in Ehrlich solid tumor in mice. *Molecular and Cellular Biochemistry, 223*, 71–80.

5. Nguyen, T., Sherratt, P. J., & Pickett, C. B. (2003). Regulatory mechanisms controlling gene expression mediated by the antioxidant response element. *Annual Review of Pharmacology and Toxicology, 43*, 233–260.

6. Jones, C. I., Zhu, H., Martin, S. F., Han, Z., Li, Y., & Alevriadou, B. R. (2007). Regulation of antioxidants and phase 2 enzymes by shear-induced reactive oxygen species in endothelial cells. *Annals of Biomedical Engineering, 35*, 683–693.

7. Asher, G., Lotem, J., Cohen, B., Sachs, L., & Shaul, Y. (2001). Regulation of p53 stability and p53-dependent apoptosis by NADH quinone oxidoreductase 1. *Proceedings of the National Academy of Sciences of the United States of America, 298,* 1188–1193.

8. Anwar, A., Dehn, D., Siegel, D., Kepa, J. K., Tang, L. J., Pietenpol, J. A., & Ross, D. (2003). Interaction of human NAD(P)H:quinone oxidoreductase 1 (NQO1) with the tumor suppressor protein p53 in cells and cell-free systems. *Journal of Biological Chemistry, 278,* 10368–10373.

9. Polyak, K., Xia, Y., Zweier, J. L., Kinzler, K. W., & Vogelstein, B. (1997). A model for p53-induced apoptosis. *Nature, 389*, 300–305.

10. Tan, M., Li, S., Swaroop, M., Guan, K., Oberley, L. W., & Sun, Y. (1999). Transcriptional activation of the human glutathione peroxidase promoter by p53. *Journal of Biological Chemistry, 274*, 12061–12120.

11. Bensaad, K., & Vousden, K. H. (2007). p53: New roles in metabolism. *Trends in Cell Biology, 17*, 286–291.

12. Siegel, D., Gustafson, D. L., Dehn, D. L., Han, J. Y., Boonchoong, P., Berliner, L. J., & Ross, D. (2004). NAD(P)H:quinone oxidoreductase 1: Role as a superoxide scavenger. *Molecular Pharmacology, 65*, 1238–1247.

13. Trush, M. A., Twerdok, L. E., Rembish, S. J., Zhu, H., & Li, Y. (1996). Analysis of target cell susceptibility as a basis for the development of a chemoprotective strategy against benzene-induced hematotoxicities. *Environmental Health Perspectives, 104*(Suppl 6), 1227–1234.

14. Siegel, D., & Ross, D. (2000). Immunodetection of NAD(P)H:quinone oxidoreductase 1 (NQO1) in human tissues. *Free Radical Biology and Medicine, 29*, 246–253.

15. Cao, Z., & Li, Y. (2004). The chemical inducibility of mouse cardiac antioxidants and phase 2 enzymes in vivo. *Biochemical and Biophysical Research Communications, 317*, 1080–1088.

16. Cao, Z., & Li, Y. (2004). Potent induction of cellular antioxidants and phase 2 enzymes by resveratrol in cardiomyocytes: Protection against oxidative and electrophilic injury. *European Journal of Pharmacology, 489*, 39–48.

17. Beall, H. D., Winski, S., Swann, E., Hudnott, A. R., Cotterill, A. S., O'Sullivan, N., Green, S. J., Bien, R., Siegel, D., & Ross, D. (1998). Indolequinone antitumor agents: Correlation between quinone structure, rate of metabolism by recombinant human NAD(P)H:quinone oxidoreductase and in vitro cytotoxicity. *Journal of Medicinal Chemistry, 41*, 4755–4766.

18. Cao, Z., Hardej, D., Trombetta, L. D., Trush, M. A., & Li, Y. (2003). Induction of cellular glutathione and glutathione S-transferase by 3*H*-1,2-dithiole-3-thione in rat aortic smooth muscle A10 cells: Protection against acrolein-induced toxicity. *Atherosclerosis, 166*, 291–301.

19. Zhu, H., Cao, Z., Zhang, L., Trush, M. A., & Li, Y. (2007). Glutathione and glutathione-linked enzymes in normal human aortic smooth muscle cells: Chemical inducibility and protection against reactive oxygen and nitrogen species-induced injury. *Molecular and Cellular Biochemistry, 301*, 47–59.

20. Zhu, H., Zhang, L., Itoh, K., Yamamoto, M., Ross, D., Trush, M. A., Zweier, J. L., & Li, Y. (2006). Nrf2 controls bone marrow stromal cell susceptibility to oxidative and electrophilic stress. *Free Radical Biology and Medicine, 41*, 132–143.

21. Zhu, H., Zhang, L., Trush, M. A., & Li, Y. (2007). Upregulation of endogenous glutathione system by 3*H*-1,2-dithiole-3-thione in pancreatic RINm5F beta-cells as a novel strategy for protecting against oxidative beta-cell injury. *Free Radical Research, 41,* 242–250.

22. Spitz, D. R., & Oberley, L. W. (1989). An assay for superoxide dismutase activity in mammalian tissue homogenates. *Analytical Biochemistry, 179,* 8–18.

23. Halford, W. P., Falco, V. C., Gebhardt, B. M., & Carr, D. J. (1999). The inherent quantitative capacity of the reverse transcription-polymerase chain reaction. *Analytical Biochemistry, 266,* 181–191.

24. Li, Y., Zhu, H., Kuppusamy, P., Roubaud, V., Zweier, J. L., & Trush, M. A. (1998). Validation of lucigenin (bis-N-methylacridinium) as a chemilumigenic probe for detecting superoxide anion radical production by enzymatic and cellular systems. *Journal of Biological Chemistry, 73,* 2015–2023.

25. Zhu, H., Itoh, K., Yamamoto, M., Zweier, J. L., & Li, Y. (2005) Role of Nrf2 signaling in regulation of antioxidants and phase 2 enzymes in cardiac fibroblasts: Protection against reactive oxygen and nitrogen species-induced cell injury. *FEBS Letter, 579,* 3029–3036.

26. Dehn, D. L., Siegel, D., Swann, E., Moody, C. J., & Ross, D. (2003). Biochemical, cytotoxic, and genotoxic effects of ES936, a mechanism-based inhibitor of NAD(P)H:quinone oxidoreductase 1, in cellular systems. *Molecular Pharmacology, 64,* 714–720.

27. Halliwell, B., & Gutteridge, J. M. C. (1999). Antioxidant defenses In B. Halliwell & J. M. C. Gutteridge (Eds.), *Free Radicals in Biology and Medicine* (3rd ed, pp. 105–245). London: Oxford University Press. .

28. Marklund, S., & Marklund, G. (1974). Involvement of the superoxide anion radical in the autoxidation of pyrogallol and a convenient assay for superoxide dismutase. *European Journal of Biochemistry 47,* 469–474.

29. Gao, R., Yuan, Z., Zhao, Z., & Gao, X. (1998). Mechanism of pyrogallol autoxidation and determination of superoxide dismutase enzyme activity. *Bioelectrochemistry and Bioenergetics, 45,* 41–45.